Genomics 93 (2009) 332–342

Contents lists available at ScienceDirect

Genomics

journal homepage: www.elsevier.com/locate/ygeno

Early whole-genome transcriptional response induced by benzo[a]pyrene diol epoxide in a normal human cell line

Xiangyun Lu [1], Jimin Shao [1], Hongjuan Li [2], Yingnian Yu *

Department of Pathology and Pathophysiology, Zhejiang University School of Medicine, Hangzhou 310058, China

ARTICLE INFO

Article history:
Received 26 June 2008
Accepted 16 December 2008
Available online 14 January 2009

Keywords:
(±)-anti-benzo[a]pyrene-7,8-diol-9,10-epoxide (BPDE)
Microarray profiling
Quantitative real-time RT-PCR
Differential gene expression
Transcriptional regulation

ABSTRACT

(±)-*anti*-benzo[a]pyrene-7,8-diol-9,10-epoxide (BPDE) is a carcinogen causing bulky-adduct DNA damage. In this study, we investigated early transcriptional signatures induced by various concentrations (0.005, 0.05, and 0.5 μM) of this carcinogen in a normal human cell line (FL human amnion epithelial cells) using the whole-genome Affymetrix HG-U133 Set microarray. The numerous identified genes were involved in multiple functions and higher doses of BPDE elicited more robust expression changes. The disturbance of genes involved in cell cycle regulation, growth and apoptosis was correlated with the S and G_2/M phase cell cycle arrest and cytotoxic phenotypes induced by different levels of BPDE. Bioinformatic analysis showed that several transcription factors and their related stress signaling pathways might partly account for the transcriptional signature induced by BPDE. Additionally, gene ontology analysis of the microarray data showed down-regulation of transport, cytoskeleton and DNA repair by 0.5 μM BPDE exposure. In conclusion, this genomic analysis helps to understand the mechanism of cellular response to BPDE.

Introduction

Polycyclic aromatic hydrocarbons (PAHs) are widespread environmental pollutants that have been found in cigarette smoke and charred food, as well as the exhaust from internal combustion engines and coal-burning factories [1]. Benzo[a]pyrene (BaP) is one of the most widely studied PAHs. It is metabolized by cytochrome P450 s to form the ultimate carcinogen, (±)-*anti*-benzo[a]pyrene-7,8-diol-9,10-epoxide (BPDE). BPDE can bind covalently to deoxyribonucleic acids (DNAs) or non-covalently intercalate into double-stranded DNA, which result in bulky-adduct DNA damage and conformational abnormalities, respectively [2]. BPDE preferentially reacts with the N^2 position of deoxyguanosine residues to form the dG-N^2-BPDE major adduct, and principally induces a G:C to T:A transversion mutation [3]. This point mutation is consistently found at the hotspot codons on the p53 gene in lung cancers from smokers but not from nonsmokers, thus implicating BPDE as the direct carcinogen accounting for cigarette smoking-induced lung cancers [4].

In recent years, genomic tools represented by microarrays have been implemented into traditional toxicology to form toxicogenomics, which involves many applications based on gene profiles, and in the end helps to understand the complex gene–toxicant interactions. For instance, gene signatures in exposure to ionizing radiation (IR) [5] and ultraviolet radiation (UV) [6] have provided insight into mutagenesis and stress response induced by these classical genotoxic agents, respectively. Gene profiling studies on BPDE have also been performed in different cell types and treatment models [7–12]. The alteration of genes involved in p53 pathway, cell cycle, cell growth, apoptosis, DNA repair, glutathione detoxification pathway and inflammation etc. have been identified, and helps to explain the cell cycle-arrest, mutagenic, cytotoxic and pro-inflammatory effect of BPDE in the related models. However, the previous *mRNA* transcriptomic studies on BPDE did not reach the whole-genome level in their used microarray or rapid analysis of gene expression (RAGE) technologies. This drawback impeded obtaining full-scale transcriptional responses induced by BPDE.

We thus used the whole-genome Affymetrix HG-U133 Set microarray that covers ~33,000 human genes and ESTs to explore responsive genes after exposure to different doses of BPDE in human amnion epithelial FL cells. We have used FL cell line as an *in vitro* model to study low doses of environmental chemical pollutants-induced responses in normal human cells for the exposure dosage to them is usually low in human daily life [1,7,13–15]. We performed genomic analysis at an early 4-h time point after BPDE exposure for early cellular changes could be useful indicators of the harmful exposure and help to understand the underlying mechanisms of chemical-caused damages, also be convenient to compare the BPDE-induced transcriptional responses with several previously reported studies being in a similar time-point context [7,8,12]. Through Affymetrix HG-U133 Set microarray analysis, we have characterized

Abbreviations: BPDE, (±)-anti-benzo[a]pyrene-7,8-diol-9,10-epoxide; AP-1, activator protein-1; NF-κB, nuclear factor kappa B; ATF, activating transcription factor; CREB, cAMP responsive element binding.

* Corresponding author. Fax: +86 571 8820 8209.
E-mail address: ynyu@zju.edu.cn (Y. Yu).
[1] These authors contributed equally to this work.
[2] Present address: Department of Basic Medicine, Hangzhou Normal University, Hangzhou 310036, China.

0888-7543/$ – see front matter © 2008 Elsevier Inc. All rights reserved.
doi:10.1016/j.ygeno.2008.12.007

the gene signatures in response to different doses (0.005, 0.05, and 0.5 μM) of BPDE. The numerous genes are involved in multiple functions including cell cycle regulation, proliferation, apoptosis, transcription, metabolism, transport, cytoskeleton and DNA repair etc. Gene ontology analysis of the microarray data using GSEA software has revealed the down-regulation of cell cycle, proliferation, transport, cytoskeleton and DNA repair by 0.5 μM BPDE exposure. A medium-throughput quantitative real-time RT-PCR validation based on TaqMan® Low-Density Array has confirmed more than one hundred of gene expression changes. The validated gene sets showed the correlation between gene expression change and the cell cycle and cytotoxicity phenotypes induced by different doses of BPDE, also provided insight into the transcriptional regulation and stress signaling pathways triggered by BPDE damage.

Results and discussion

Early global changes in gene expression after BPDE treatment

Three concentrations of BPDE (0.005, 0.05, and 0.5 μM) were used to treat human amnion epithelial FL cells for the microarray profiling study. 0.005 and 0.05 μM BPDE did not affect cell viability evidently and 0.5 μM BPDE produced a moderate cytotoxicity (88% cell viability) compared with DMSO vehicle exposure as determined by MTT reduction assay (Fig. 1). With Affymetrix HG-U133 Set microarray analysis, we found that the expression of 74, 103, and 2176 probe sets representing 70 (31 up- and 39 down-regulated), 88 (38 up- and 50 down-regulated), and 1707 (307 up- and 1400 down-regulated) genes were significantly altered at 4 h after exposure to 0.005, 0.05, and 0.5 μM BPDE, respectively, compared with the vehicle exposure (Supplementary Table 1). These profiles constituted a total of 1764 unique genes that were differentially expressed in at least one of the three concentrations of BPDE treatment. Hierarchical clustering of the 1764 genes based on their fold changes relative to the control was performed to visualize the change patterns with the two biological replicates separated (Fig. 2a). It could be cognized that the microarray profiling replication was acceptable with the replicate samples clustered most close, and the 0.5 μM BPDE provoked much more extensive transcriptional changes than the two lower doses did.

Affymetrix gene ontology annotation showed that the differentially expressed genes were involved in multiple biological functions such as cell cycle regulation, signal transduction, transcription, translation, metabolism, transport, cytoskeleton, DNA repair, and etc. (Supplementary Table 1). We further used Gene Set Enrichment Analysis (GSEA) software to analyze whether some functional categories of genes were significantly enriched in the differentially expressed dataset, and coordinately regulated to enhance or impair some cellular activities after BPDE treatment. By searching the mSigDB gene ontology gene set collection, GSEA analysis filtered out 233 gene sets in the 0.5 μM BPDE dataset, 1 gene set in the 0.05 μM BPDE dataset, and none in the lowest dose dataset. The enriched gene sets in the 0.5 μM BPDE group were also mainly involved in cell cycle, proliferation, apoptosis, signal transduction, transcription, RNA processing, protein metabolism, transport, cytoskeleton, and DNA repair etc. (Supplementary Table 2). These identified gene expression changes prominently indicated down-regulation of cell cycle, proliferation, transport, cytoskeleton, and DNA repair (Supplementary Fig. 1).

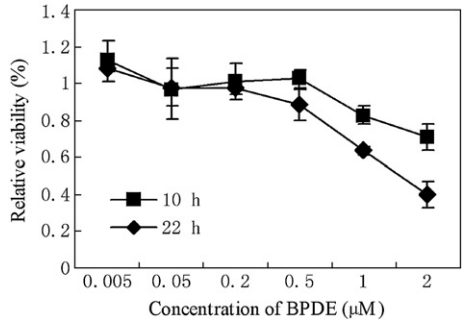

Fig. 1. Cell viability measured by MTT assay. Human amnion epithelial FL cells were exposed to different concentrations of BPDE for 2 h. At 10 and 22 h after exposure, cell viability for each treatment was determined based on spectrometry of formazan formation, and relative viability represented the viability percentage relative to vehicle exposure. Triplicate experiments were carried out, and $\bar{x}$±SD was calculated for diagram.

Quantitative real-time RT-PCR validation

A medium-scale quantitative real-time RT-PCR validation of the microarray results based on TaqMan® Low-Density Array was performed using independently prepared cell samples. Of 35, 47, and 234 responsive genes selected from 0.005, 0.05 and 0.5 μM BPDE-treated samples, 7, 16, and 111 genes showed same change trends in their expression as that identified by microarray analysis. Among which, 2, 6, and 57 genes were confirmed with statistical significance ($p<0.05$). The validated gene list covers many functional categories, and includes many genes related with cell cycle regulation, proliferation, apoptosis, transcription, metabolism, transport, cytoskeleton, and DNA repair etc. (Table 1 and Fig. 2b).

Dose effect of BDPE on cell cycle regulation

Microarray analysis revealed an early alteration in expression of numerous cell cycle-regulating genes after BPDE treatment. A portion of these genes was selected and validated by quantitative RT-PCR (Table 1). Following 0.05 and 0.5 μM BPDE treatment, the expression of *H1F0* (H1 histone family, member 0), *AURKA* (aurora kinase A), *CCNB1* (cyclin B1), and *CENPA* (centromere protein A) was decreased. The down-regulation of *H1F0* implied slow down of DNA synthesis [16], and the decreased expression of the other three genes that function in promoting G_2/M progression indicated G_2/M blockade [17–19]. Upon 0.5 μM BPDE exposure, the expression of four more genes was affected, among which three genes that act in promoting G_2/M progression including *CDC20* (cell division cycle 20 homolog) [20], *KIF14* (kinesin family member 14) [21], and *KIF2C* (kinesin family member 2C) [22] were down-regulated, and one gene that functions in blocking the onset of mitosis, i.e., *PKMYT1* (protein kinase, membrane-associated tyrosine/threonine 1) [23], was up-regulated. These gene expression changes indicate that 0.5 μM BPDE induced a more potently inhibition of G_2/M progression compared with 0.05 μM BPDE treatment. No gene expression changes related to cell cycle regulation was validated by quantitative RT-PCR in 0.005 μM BPDE-treated samples.

Flow cytometry assay was performed to explore the correlation between these gene expression changes and cell cycle phenotype. Cell cycle distributions were recorded at 4, 13, and 22 h post BPDE treatment (Fig. 3). 0.05 μM BPDE elicited S phase delay as early as at 4 h post treatment and caused G_2/M arrest later as identified at 13 h and 22 h post treatment. 0.5 μM BPDE evoked much more severe S phase delay than 0.05 μM BPDE at all three time points. The S phase-delayed cells induced by 0.5 μM BPDE were partially released but still arrested at G_2/M transition at 22 h post treatment. The G_1 peak diminished at 22 h after 0.5 μM BPDE treatment, indicating a more profound S phase and G_2/M blockade was triggered compared with 0.05 μM BPDE treatment. The 0.005 μM BPDE seemed to only elicit much milder G_2/M arrest as late as at 13 and 22 h post treatment. Thus, these data showed the consistency of gene expression change with cell cycle phenotype and the dose effect of BDPE on the down-regulation of cell cycle progression.

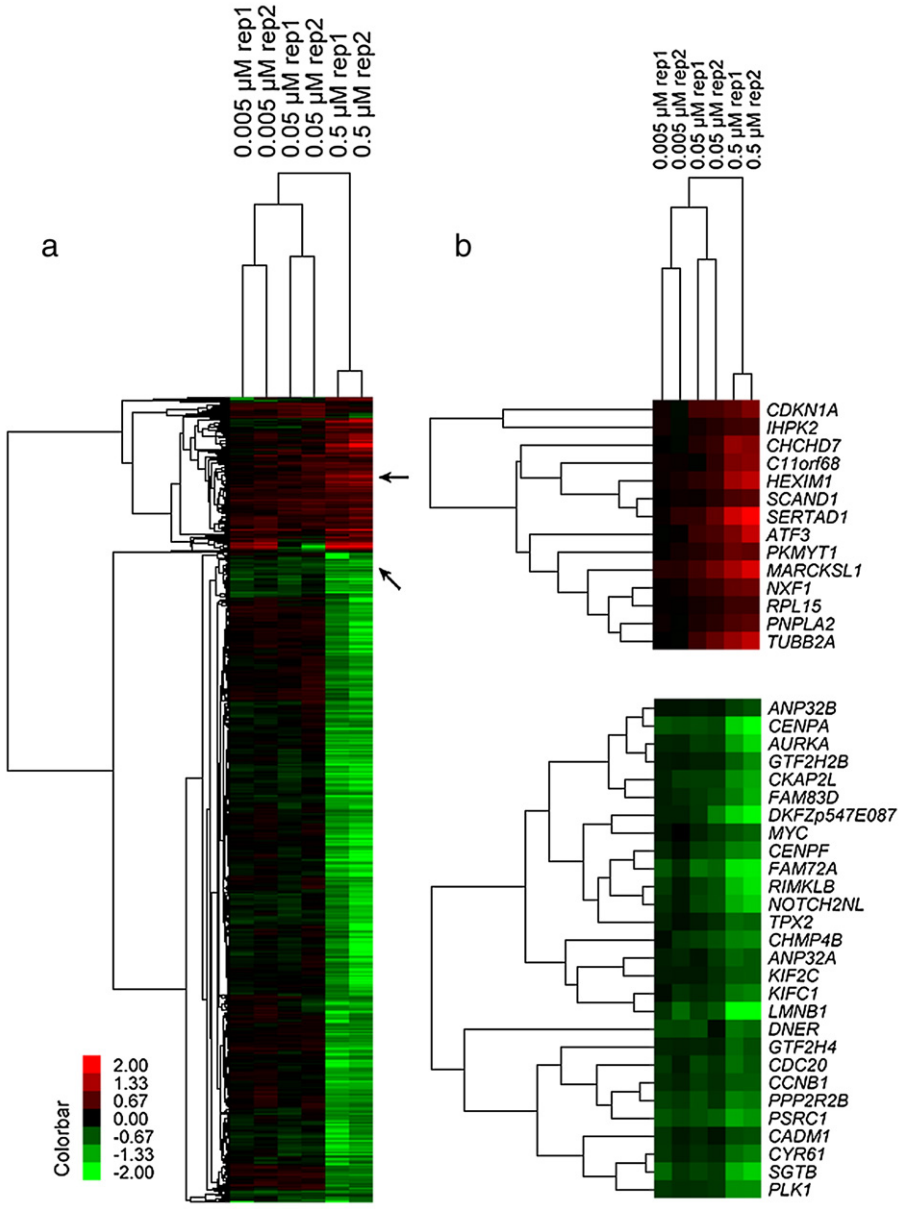

Fig. 2. (a) Hierarchical clustering analysis. Hierarchical clustering of the 1764 genes that differentially expressed in at least one of the three doses of BPDE treatment was performed with the two biological replicates separated. Experimental conditions are on the horizontal axis and affected genes are grouped along the vertical axis. Gene expression changes are colored red for up-regulation or green for down-regulation. The scale of colorbar was ranged from −2 to 2, representing 4-fold change of down and up-regulation, respectively. (b) Enlargement of two clusters (arrow pointed) in the dendrogram. Among which, a dozen genes involved in cell cycle, proliferation and apoptosis, etc. have been validated by quantitative RT-PCR.

In respond to 0.5 μM BPDE treatment *CDKN1A* (cyclin-dependent kinase inhibitor 1A (p21, Cip1)) and *CDKN1C* (cyclin-dependent kinase inhibitor 1C (p57, Kip2)) were induced, and *CDK6* (cyclin-dependent kinase 6) was repressed, which would lead to the impairment of G_1/S transition [24]. However, the simultaneous up-regulation of *CCNE1* (cyclin E1) and *CCNE2* (cyclin E2) could enhance G_1/S transition [24]. Cell cycle analysis showed that a G_1/S arrest was not established upon all three doses of BPDE treatment (Fig. 3).

Responsive genes and related pathways involved in cell growth and apoptosis

Important genes including membrane receptors, signaling molecules, and transcription factors that determine cell fate were affected by 0.5 μM BPDE at 4 h post treatment. These included repression of *EGFR* (epidermal growth factor receptor) and *IGF1R* (insulin-like growth factor 1 receptor), both of which belong to single-transmembrane receptor tyrosine kinases (RTK). Physiological binding of ligands to these receptors leads to activation of phosphatidylinositol-3-kinase (PI3K)/Akt, Ras/MAPK (mitogen-activated protein kinase), and phospholipase C (PLCγ)-mediated pathways, which regulate a wide variety of downstream targets related with cell metabolism, migration, proliferation, differentiation, and survival [25]. Downstream of the PLCγ-mediated pathways were also affected. PLCγ catalyzes PtdIns(4,5)P_2 to generate second messengers including diacylglycerol (DAG) and Ins(1,4,5)P_3 (IP_3). DAG activates protein kinase C (PKC). IP_3 induces Ca^{2+} release from the calcium pool by binding to the ion channel receptor ITPR1 (inositol 1,4,5-triphosphate receptor type 1)/IP3R. The released Ca^{2+} binds with calmodulin, thereby activating Ca^{2+}/calmodulin-dependent protein kinases (CaMKs) [25]. Upon 0.5 μM BPDE treatment, the expression of *PRKCA* (protein kinase C, alpha) and *ITPR1* were reduced. Thus, the down-

Table 1
Validation of gene expression changes at 4 h post BPDE treatment with quantitative real-time RT-PCR

RefSeq ID	Probe ID	Gene title	Gene symbol	Fold change	
				Array	PCR
0.005 μM BPDE					
Regulation of transcription					
NM_153207	225889_at	AE binding protein 2	*AEBP2*	−1.34	−1.35
NM_001271	228999_at	Chromodomain helicase DNA binding protein 2	*CHD2*	−1.78	−1.28
Signal transduction					
NM_016441	228496_s_at	Cysteine rich transmembrane BMP regulator 1 (chordin-like)	*CRIM1*	−1.23	−1.20
NM_001901	209101_at	Connective tissue growth factor	*CTGF*	−1.33	−1.20
NM_139072	226281_at	Delta/notch-like EGF repeat containing	*DNER*	−1.46	−1.35*
Membrane trafficking					
NM_001283	205196_s_at	Adaptor-related protein complex 1, sigma 1 subunit	*AP1S1*	−1.52	−1.29*
Solute transport					
NM_016612	221920_s_at	Solute carrier family 25, member 37	*SLC25A37*	1.95	1.21
0.05 μM BPDE					
Regulation of transcription					
NM_006305	201043_s_at	Acidic (leucine-rich) nuclear phosphoprotein 32 family, member A	*ANP32A*	−1.23	−1.71
NM_001913	214743_at	Cut-like homeobox 1	*CUX1*	−1.52	−1.62
Cell cycle regulation					
NM_003600	208079_s_at	Aurora kinase A	*AURKA*	−1.50	−1.70
NM_031966	228729_at	Cyclin B1	*CCNB1*	−1.36	−1.87*
NM_001809	204962_s_at	Centromere protein A	*CENPA*	−1.48	−3.21
NM_005318	208886_at	H1 histone family, member 0	*H1F0*	−1.89	−1.98
Signal transduction					
NM_016441	228496_s_at	Cysteine rich transmembrane BMP regulator 1 (chordin-like)	*CRIM1*	−1.32	−1.35
NM_001901	209101_at	Connective tissue growth factor	*CTGF*	−1.62	−1.59*
NM_001554	201289_at	Cysteine-rich, angiogenic inducer, 61	*CYR61*	−1.26	−1.41
NM_139072	226281_at	Delta/notch-like EGF repeat containing	*DNER*	−1.28	−1.45*
Protein folding					
NM_014260	233588_x_at	Prefoldin subunit 6	*PFDN6*	−1.40	−1.93
Membrane trafficking					
NM_001283	205196_s_at	Adaptor-related protein complex 1, sigma 1 subunit	*AP1S1*	−1.58	−1.52*
NM_014914	204066_s_at	ArfGAP with GTPase domain, ankyrin repeat and PH domain 1	*AGAP1*	−1.39	−1.90*
Unknown					
NM_001620	235281_x_at	AHNAK nucleoprotein	*AHNAK*	−1.57	−1.48
NM_030919	225687_at	Family with sequence similarity 83, member D	*FAM83D*	−1.40	−2.39*
NM_018386	225149_at	PCI domain containing 2	*PCID2*	−1.34	−1.35
0.5 μM BPDE					
Regulation of transcription					
NM_153207	225889_at	AE binding protein 2	*AEBP2*	−4.13	−1.24*
NM_020731	229354_at	Aryl-hydrocarbon receptor repressor	*AHRR*	−2.01	−3.00
NM_013275	238538_at	Ankyrin repeat domain 11	*ANKRD11*	−3.45	−1.74*
NM_001674	202672_s_at	Activating transcription factor 3	*ATF3*	2.39	1.67*
NM_004824	203098_at	Chromodomain protein, Y-like	*CDYL*	−4.35	−1.27**
NM_001913	214743_at	Cut-like homeobox 1	*CUX1*	−2.41	−2.10**
NM_006460	202814_s_at	Hexamethylene bis-acetamide inducible 1	*HEXIM1*	2.58	1.96
NM_002398	204069_at	Meis homeobox 1	*MEIS1*	−2.75	−2.06*
NM_002467	202431_s_at	v-myc myelocytomatosis viral oncogene homolog (avian)	*MYC*	−1.64	−1.31
NM_002518	205460_at	Neuronal PAS domain protein 2	*NPAS2*	−2.13	−1.66
NM_003298	225477_s_at	Nuclear receptor subfamily 2, group C, member 2	*NR2C2*	−3.23	−1.27
NM_005870	208740_at	Sin3A-associated protein, 18 kDa	*SAP18*	2.02	1.61
NM_021961	214600_at	TEA domain family member 1 (SV40 transcriptional enhancer factor)	*TEAD1*	−2.75	−1.80
NM_014943	203556_at	Zinc fingers and homeoboxes 2	*ZHX2*	−11.06	−1.76*
Cell cycle regulation					
NM_003600	204092_s_at	Aurora kinase A	*AURKA*	−2.78	−3.31*
NM_031966	214710_s_at	Cyclin B1	*CCNB1*	−1.64	−1.64*
NM_001238	213523_at	Cyclin E1	*CCNE1*	1.86	1.59*
NM_057735	205034_at	Cyclin E2	*CCNE2*	1.67	2.18*
NM_001255	202870_s_at	Cell division cycle 20 homolog (*S. cerevisiae*)	*CDC20*	−1.71	−1.65*
NM_001259	207143_at	Cyclin-dependent kinase 6	*CDK6*	−2.93	−1.55*
NM_000389	202284_s_at	Cyclin-dependent kinase inhibitor 1A (p21, Cip1)	*CDKN1A*	1.81	1.36
NM_000076	213182_x_at	Cyclin-dependent kinase inhibitor 1C (p57, Kip2)	*CDKN1C*	1.46	1.23
NM_001809	204962_s_at	Centromere protein A	*CENPA*	−3.95	−2.23**
NM_005318	208886_at	H1 histone family, member 0	*H1F0*	−2.37	−2.04*
NM_014875	206364_at	Kinesin family member 14	*KIF14*	−3.01	−1.49

(continued on next page)

Table 1 (*continued*)

RefSeq ID	Probe ID	Gene title	Gene symbol	Fold change	
				Array	PCR
0.5 μM BPDE					
Cell cycle regulation					
NM_006845	211519_s_at	Kinesin family member 2C	*KIF2C*	−1.60	−1.55*
NM_014572	227013_at	LATS, large tumor suppressor, homolog 2 (*Drosophila*)	*LATS2*	−3.05	−1.80*
NM_003550	204857_at	MAD1 mitotic arrest deficient-like 1 (yeast)	*MAD1L1*	−2.04	−1.90
NM_004203	204267_x_at	Protein kinase, membrane associated tyrosine/threonine 1	*PKMYT1*	1.72	1.70*
Signal transduction					
NM_006738	221718_s_at	A kinase (PRKA) anchor protein 13	*AKAP13*	−4.97	−2.61*
NM_173075	213419_at	Amyloid beta (A4) precursor protein-binding, family B, member 2 (Fe65-like)	*APBB2*	−18.60	−3.03*
NM_006888	200653_s_at	Calmodulin 1 (phosphorylase kinase, delta)	*CALM1*	1.25	1.31
NM_016441	202551_s_at	Cysteine rich transmembrane BMP regulator 1 (chordin-like)	*CRIM1*	−2.08	−1.55**
NM_001554	201289_at	Cysteine-rich, angiogenic inducer, 61	*CYR61*	−1.91	−1.29*
NM_004087	202514_at	Discs, large homolog 1 (*Drosophila*)	*DLG1*	−2.99	−1.33
NM_005228	201983_s_at	Epidermal growth factor receptor (erythroblastic leukemia viral (v-erb-b) oncogene homolog, avian)	*EGFR*	−2.61	−2.05*
NM_004864	221577_x_at	Growth differentiation factor 15	*GDF15*	3.41	2.45*
NM_001945	203821_at	Heparin-binding EGF-like growth factor	*HBEGF*	3.14	1.25*
NM_000875	203627_at	Insulin-like growth factor 1 receptor	*IGF1R*	−3.16	−2.10*
NM_002222	203710_at	Inositol 1,4,5-triphosphate receptor, type 1	*ITPR1*	−2.62	−1.92*
NM_005923	203836_s_at	Mitogen-activated protein kinase kinase kinase 5	*MAP3K5*	−3.67	−1.50
NM_003791	201620_at	Membrane-bound transcription factor peptidase, site 1	*MBTPS1*	−1.67	−1.50**
NM_145117	218330_s_at	Neuron navigator 2	*NAV2*	−3.75	−2.49*
NM_014840	204589_at	NUAK family, SNF1-like kinase, 1	*NUAK1*	−3.32	−1.39
NM_002581	224940_s_at	Pregnancy-associated plasma protein A, pappalysin 1	*PAPPA*	−4.06	−1.68*
NM_000921	206389_s_at	Phosphodiesterase 3A, cGMP-inhibited	*PDE3A*	−3.95	−1.72
NM_006457	203242_s_at	PDZ and LIM domain 5	*PDLIM5*	−3.38	−1.83
NM_003768	200788_s_at	Phosphoprotein enriched in astrocytes 15	*PEA15*	1.56	1.60
NM_025179	213030_s_at	Plexin A2	*PLXNA2*	−3.27	−2.11
NM_002737	215195_at	Protein kinase C, alpha	*PRKCA*	−2.92	−2.17*
NM_004249	209084_s_at	RAB28, member RAS oncogene family	*RAB28*	−1.97	−1.45
NM_032730	224509_s_at	Reticulon 4 interacting protein 1	*RTN4IP1*	−5.13	−1.44*
NM_003246	201108_s_at	Thrombospondin 1	*THBS1*	−1.69	−1.51
NM_007118	208178_x_at	Triple functional domain (PTPRF interacting)	*TRIO*	−3.21	−1.87
NM_003371	205537_s_at	Vav 2 guanine nucleotide exchange factor	*VAV2*	−8.18	−2.52*
Metabolism					
NM_014324	209425_at	Alpha-methylacyl-CoA racemase	*AMACR*	1.54	1.81*
NM_024830	201818_at	Lysophosphatidylcholine acyltransferase 1	*LPCAT1*	−7.50	−1.17*
NM_000104	202434_s_at	Cytochrome P450, family 1, subfamily B, polypeptide 1	*CYP1B1*	2.95	1.57*
NM_020474	201722_s_at	UDP-N-acetyl-alpha-D-galactosamine:polypeptide N-acetylgalactosaminyltransferase 1 (GalNAc-T1)	*GALNT1*	−1.81	−1.46
NM_017423	218313_s_at	UDP-N-acetyl-alpha-D-galactosamine:polypeptide N-acetylgalactosaminyltransferase 7 (GalNAc-T7)	*GALNT7*	−2.08	−1.28*
NM_147175	230030_at	Heparan sulfate 6-O-sulfotransferase 2	*HS6ST2*	−2.91	−1.86
NM_015440	225520_at	Methylenetetrahydrofolate dehydrogenase (NADP+ dependent) 1-like	*MTHFD1L*	−2.76	−1.84
NM_000434	208926_at	Sialidase 1 (lysosomal sialidase)	*NEU1*	1.73	1.61**
NM_020376	212705_x_at	Patatin-like phospholipase domain containing 2	*PNPLA2*	1.57	1.28
NM_002970	203455_s_at	Spermidine/spermine N1-acetyltransferase 1	*SAT1*	2.94	1.68
NM_024636	220187_at	STEAP family member 4	*STEAP4*	−1.74	−1.12
DNA replication					
NM_002897	203748_x_at	RNA binding motif, single stranded interacting protein 1	*RBMS1*	−3.28	−1.71
DNA repair					
NM_002874	223598_at	RAD23 homolog B (S. cerevisiae)	*RAD23B*	−2.15	−1.53*
RNA processing					
NM_005463	209067_s_at	Heterogeneous nuclear ribonucleoprotein D-like	*HNRPDL*	−2.13	−1.59
NM_006362	208922_s_at	Nuclear RNA export factor 1	*NXF1*	1.75	1.98
NM_006275	208804_s_at	Splicing factor, arginine/serine-rich 6	*SFRS6*	1.62	1.30
Protein synthesis					
NM_003750	200596_s_at	Eukaryotic translation initiation factor 3, subunit A	*EIF3A*	−1.86	−1.10
NM_002094	215438_x_at	G1 to S phase transition 1	*GSPT1*	−1.65	−1.61*
Protein catabolism					
NM_031483	239101_at	Itchy homolog E3 ubiquitin protein ligase (mouse)	*ITCH*	−10.07	−1.53
NM_174916	226921_at	Ubiquitin protein ligase E3 component n-recognin 1	*UBR1*	−3.33	−1.34
Cytoskeleton					
NM_020806	220773_s_at	Gephyrin	*GPHN*	−1.98	−2.73*
NM_005573	203276_at	Lamin B1	*LMNB1*	−4.17	−1.37

Table 1 (*continued*)

RefSeq ID	Probe ID	Gene title	Gene symbol	Fold change	
				Array	PCR
0.5 μM BPDE					
Cytoskeleton					
NM_022818	208785_s_at	Microtubule-associated protein 1 light chain 3 beta	*MAP1LC3B*	1.38	1.32
NM_023009	200644_at	MARCKS-like 1	*MARCKSL1*	2.85	1.70
NM_001069	204141_at	Tubulin, beta 2A	*TUBB2A*	2.53	1.63
Membrane trafficking					
NM_001283	205196_s_at	Adaptor-related protein complex 1, sigma 1 subunit	*AP1S1*	−1.59	−1.17
NM_014914	204066_s_at	ArfGAP with GTPase domain, ankyrin repeat and PH domain 1	*AGAP1*	−3.94	−2.99**
NM_003024	209297_at	intersectin 1 (SH3 domain protein)	*ITSN1*	−2.70	−1.56*
Solute transport					
NM_004694	207038_at	Solute carrier family 16, member 6 (monocarboxylic acid transporter 7)	*SLC16A6*	−1.99	−1.30
NM_052885	227176_at	Solute carrier family 2 (facilitated glucose transporter), member 13	*SLC2A13*	−3.08	−1.38
Immune response					
NM_005516	200904_at	Major histocompatibility complex, class I, E	*HLA-E*	1.61	1.45*
NM_003811	206907_at	Tumor necrosis factor (ligand) superfamily, member 9	*TNFSF9*	1.51	1.71*
NM_025217	238542_at	UL16 binding protein 2	*ULBP2*	1.49	2.30*
Unknown					
NM_007011	63825_at	Abhydrolase domain containing 2	*ABHD2*	−1.81	−1.50*
NM_019004	224682_at	Ankyrin repeat and IBR domain containing 1	*ANKIB1*	−2.26	−1.60*
NM_031450	221534_at	Chromosome 11 open reading frame 68	*C11orf68*	2.04	1.21
NM_138425	224719_s_at	Chromosome 12 open reading frame 57	*C12orf57*	1.67	1.38
NM_033286	225300_at	Chromosome 15 open reading frame 23	*C15orf23*	−2.66	−1.73**
NM_020317	209006_s_at	Chromosome 1 open reading frame 63	*C1orf63*	3.66	1.51
XR_017929	230251_at	Chromosome 6 open reading frame 176	*C6orf176*	−4.55	−2.08*
NM_152515	229610_at	Cytoskeleton associated protein 2-like	*CKAP2L*	−2.31	−1.60
NM_017993	219501_at	Ecto-NOX disulfide-thiol exchanger 1	*ENOX1*	−2.55	−3.38**
NM_153690	227410_at	Family with sequence similarity 43, member A	*FAM43A*	1.84	1.50*
NM_016605	218023_s_at	Family with sequence similarity 53, member C	*FAM53C*	2.51	1.64*
NM_030919	225687_at	Family with sequence similarity 83, member D	*FAM83D*	−2.27	−1.72*
NM_022763	218618_s_at	Fibronectin type III domain containing 3B	*FNDC3B*	−4.77	−2.38**
NM_017640	230793_at	Leucine rich repeat containing 16A	*LRRC16A*	−2.54	−1.98*
NM_019606	219798_s_at	Methylphosphate capping enzyme	*MEPCE*	1.38	1.38
NM_007211	225946_at	Ras association (RalGDS/AF-6) domain family 8	*RASSF8*	−3.10	−1.24*
NM_006997	202289_s_at	Transforming, acidic coiled-coil containing protein 2	*TACC2*	−3.88	−1.48
NM_020147	219596_at	THAP domain containing 10	*THAP10*	1.68	1.37
NM_032021	223595_at	Transmembrane protein 133	*TMEM133*	−9.66	−2.01
NM_031442	209656_s_at	Transmembrane protein 47	*TMEM47*	1.47	1.59
NM_032883	228737_at	TOX high mobility group box family member 2	*TOX2*	−3.15	−1.50
NM_015285	212880_at	WD repeat domain 7	*WDR7*	−6.12	−1.72
NM_016061	217783_s_at	Yippee-like 5 (*Drosophila*)	*YPEL5*	1.38	1.15

"*" and "**" represent $p<0.05$ and <0.01, respectively, compared with vehicle treatment (Student's paired, two-tailed *t*-test analysis).

regulation of the RTK signaling pathways by BPDE would have a negative effect on cell growth.

Two important signaling genes, *GDF15* (growth differentiation factor 15) and *PEA15* (phosphoprotein enriched in astrocytes 15), were up-regulated upon 0.5 μM BPDE treatment. *GDF15* is a member of the TGF-beta superfamily, and induced by many stress stimuli including DNA damage [5]. Its expression was correlated with increased apoptosis in some cell types [26]. *PEA15* encodes a protein characterized with an ERK1/2 binding domain and a nuclear export sequence [27]. It can repress ERK1/2 activity by sequestration of ERK1/2 at cytoplasm, thus decreased ERK1/2-dependent transcription and slowed down cell proliferation. The altered expression of these two genes induced by BPDE would disturb cell proliferation and apoptosis.

The expression of many transcription regulators (TFs) was altered upon 0.5 μM BPDE treatment (Table 1). Among which included up-regulation of *ATF3* (activating transcription factor 3) and *HEXIM1* (hexamethylene bis-acetamide inducible 1), and down-regulation of *MYC* (v-myc myelocytomatosis viral oncogene homolog (avian)). *ATF3* is induced by a wide variety of stress signals, and its induction is correlated with cellular injury [28]. Over-expression of ATF3 often leads to detrimental consequences [28]. The *HEXIM1* protein, in association with 7SK snRNA, binds and inhibits the kinase activity of P-TEFb (CDK9/CyclinT). P-TEFb activity is crucial for efficient RNA polymerase II-dependent transcription elongation. Up-regulation of *HEXIM1* mRNA and protein is a program for differentiation, and can cause growth inhibition in several cell types [29]. The *MYC* oncoprotein regulates numerous target genes involved in cell cycle, metabolism, protein synthesis, cell growth, and apoptosis [30]. Deregulation of this gene was associated with cellular apoptosis [31]. Thus, the alteration of these genes might affect cell growth, proliferation, differentiation, and apoptosis.

The metabolism gene *SAT1* (spermidine/spermine N1-acetyltransferase 1) was up-regulated upon 0.5 μM BPDE treatment (Table 1). *SAT1* encodes a rate-limiting enzyme in polyamine catabolism. Reduction of polyamine level by *SAT1* was shown to promote apoptosis and inhibit cell growth [32]. Its up-regulation by BPDE treatment possibly indicated a tendency of apoptosis and growth suppression.

These data demonstrate that 0.5 μM BPDE had profound impacts on many aspects of the cellular processes through regulating gene expression and related signal transduction. The overall effects of BPDE were to down-regulate the cell growth and activate apoptosis at early stage although MTT assay showed the cellular viability was only moderately affected.

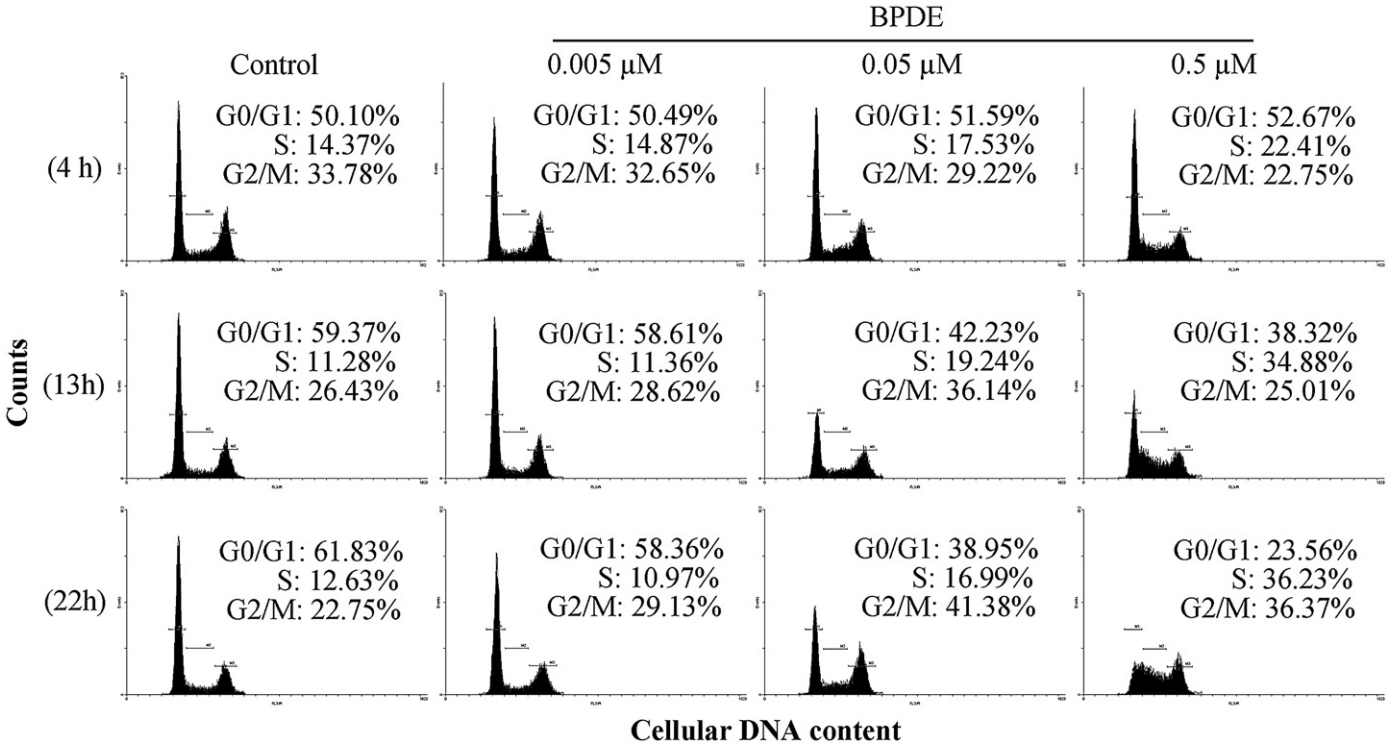

Fig. 3. Cell cycle analysis. Human amnion epithelial FL cells were exposed to various concentrations of BPDE for 2 h. At 4, 13 and 22 h post exposure, cells were collected, fixed, stained with propidium iodide, and acquired on a Coulter EPICS XL flow cytometer. Triplicate experiments were carried out, and one of which was displayed as a representative. For each cell cycle profile graph, the *x* axis represented FL3-PI fluorescence value that maximized at 1024 channels, and the *y* axis represented cell counts that maximized at 512.

Transcriptional regulation of the affected genes targeted by stress signaling pathways

Analysis of the promoters of the affected genes would help to predict corresponding TFs with changes in both expression levels and activities and their related signaling pathways. 36 up-regulated genes in response to 0.5 μM BPDE were validated with quantitative RT-PCR (Table 1). By computer-assisted prediction, TFs known to be downstream of various stress signaling pathways were picked out, thereby generated stress response-enriched TF profiles for 24 up-regulated genes (Table 2). The prominent transactivators for these affected genes were the AP-1 family TFs (AP-1, FOS and ATF2: JUN

Table 2
Prediction of transcription factors activated by 0.5 μM BPDE treatment[a]

Gene Symbol	Fold change		Predicted transcription factors	Gene function
	Array	PCR		
ATF3	2.39	1.67*	ATF4, AP-1, FOS, REL	Transcription factor
CDKN1A	1.81	1.36	AP-1, TP53, ATF3	Cell cycle arrest, inhibit G_1/S transition
CDKN1C	1.46	1.23	ATF6, ELK1	Cell cycle arrest, inhibit G_1/S transition
PKMYT1	1.72	1.70*	ATF4, AP-1	Cell cycle arrest, inhibit G_2/M transition
CALM1	1.25	1.31	AP-1, ATF2, FOS, ELK1	Calmodulin
GDF15	3.41	2.45*	TP53, NFKB1	TGFβ family member
HBEGF	3.14	1.25*	AP-1, ATF4, FOS	Growth factor
PEA15	1.56	1.60	NFKB1, TP53	Sequestration of ERKs at cytoplasm
CYP1B1	2.95	1.57*	CREB1	Xenobiotic and lipid metabolism
NEU1	1.73	1.61**	FOS	Cleavage of terminal sialic acid residues
PNPLA2	1.57	1.28	ATF6, ATF2:JUN, CREB1, ATF3, ELK1, TP53	Lipid metabolism
SAT1	2.94	1.68	ATF2	Amino acid metabolism
NXF1	1.75	1.98	ATF4	RNA export from nucleus
SFRS6	1.62	1.30	ATF-1, ATF3	RNA splicing
MAP1LC3B	1.38	1.32	CREB1	Microtubule assembly
MARCKSL1	2.85	1.70	CREB1, NF-kappaB	Actin cytoskeleton dynamics
TUBB2A	2.53	1.63	CREB1, AP-1, ATF2:JUN	Constituent of cytoskeleton
TNFSF9	1.51	1.71*	NFKB1, Chop-cEBP	Immune response
C11orf68	2.04	1.21	ATF4, CREB1, NFKB1	Unknown
C12orf57	1.67	1.38	ELK1, ATF6	Unknown
FAM43A	1.84	1.50*	RELA, REL, FOS	Unknown
THAP10	1.68	1.37	ATF3	Unknown
TMEM47	1.47	1.59	CREB1, ATF2, ATF4	Unknown
YPEL5	1.38	1.15	CREB1, AP-1, ELK1, ATF4	Unknown

[a] The Promoter Analysis Pipeline web application suite was used to identify regulatory transcription factors for up-regulated genes induced by 0.5 μM BPDE. Those transactivators related to stress response were displayed in order of their prediction probability from left to right. The "*" and "**" denote $p<0.05$ and <0.01, respectively, compared with vehicle treatment (Student's paired, two-tailed *t*-test analysis).

heterodimer), the ATF/CREB family members (CREB1, ATF4, ATF6 and ATF3), NF-κB with its subunits (NFKB1, RELA and REL), TP53, and ELK1.

Among these predicted TFs, previous studies had confirmed that AP-1, ATF3, NF-κB, TP53, and ELK1 could be activated by BPDE in various cell types [12,33–35]. The upstream signaling pathways for activation of these TFs were the MAPKs (ERKs, JNKs, p38) pathways for activating AP-1, the JNK/SAPK pathway for ATF3 accumulation and activation, the phosphorylation and degradation of IκBα for stimulating NF-κB, the ATM/ATR, ERKs, and p38 MAPKs for activating TP53, and the ERKs pathway for activating ELK1. The targeted genes included *CDKN1A*, *CDKN1C*, *PKMYT1*, *ATF3*, *SAT1*, *GDF15*, *PEA15*, and etc. (Table 2). As mentioned above, the up-regulation of these genes would impede cell cycle progression, inhibit cell growth, and promote apoptosis.

The predicted activation of ATF/CREB family members (such as CREB1, ATF4, and ATF6) by BPDE has not been reported before. CREB1 is a phosphorylation-dependent TF that can be activated by MAPKs, CaMKs, Akt, and protein kinase A (PKA) [36]. Four up-regulated genes upon 0.5 μM BPDE treatment were predicted to be targeted by CREB1 regulators, including three cytoskeleton-related genes, i.e. *MARCKSL1* (MARCKS-like) [37], *MAP1LC3B* (microtubule-associated protein 1 light chain 3 beta) [38], and *TUBB2A* (tubulin, beta 2A) [39], and one metabolism gene, i.e. *CYP1B1* (cytochrome P450, family 1, subfamily B, polypeptide 1). These cytoskeleton-related genes were not known involved in cellular response to BPDE exposure before. *CYP1B1* is an enzyme involved in metabolizing procarcinogens including polycyclic aromatic hydrocarbons [40]. The induction of *CYP1B1* by benzo[a] pyrene (BaP) was well-known [40], and BPDE is one of the ultimate carcinogens of BaP.

Both ATF4 and ATF6 were known involved in endoplasmic reticulum (ER) stress [41]. Following the initiation of ER stress, ATF4 is translationally activated by EIF2AK3 (PERK) kinase-mediated phosphorylation of eukaryotic initiation factor 2 alpha (eIF2α), while ATF6 is post-translationally capacitated following sequential cleavage by MBTPS1 (membrane-bound transcription factor peptidase, site 1) and MBTPS2. After activation, ATF4 regulates the expression of genes involved in oxidative stress resistance, and ATF6 enhances the production of molecular chaperons such as HSPA5 (GRP78/BiP), HERPUD1 (Herp), and DNAJC3 ($P58^{IPK}$), thereby mediating protective roles for cells. Both TFs also induce the expression of the pro-apoptotic protein DDIT3 (GADD153/CHOP). Our lab previously found that the protein level of HSPA5 and DDIT3 was up-regulated upon BPDE treatment [13]. These evidences support that BPDE may trigger ER stress response, in which ATF4 and ATF6 are involved. In this study, we found that several ATF4- and ATF6- targeted genes, such as *ATF3*, *PKMYT1*, *CDKN1C*, and etc. were activated in response to BPDE treatment, which could lead to down-regulation of cell cycle and cell growth (Table 2). Furthermore, we previously showed that another DNA-damaging alkylating agent, N-methyl-N′-nitro-N-nitrosoguanidine (MNNG), could activate a cAMP-PKA-CREB signaling pathway in vero cells [42] and ER stress in FL cells [14], implying that the activation of ATF/CREB TFs and ER stress could be a common mechanism of cellular response to chemical genotoxic agents.

In this study, we have investigated genome-wide transcriptional response by DNA microarray at an early stage after exposure to different levels of the mutagen and carcinogen BPDE in human amnion epithelial FL cells. More than a hundred of gene expression changes were validated with quantitative real-time RT-PCR. These early responsive genes belong to multiple functional categories. The 0.5 μM BPDE elicited much more extensive transcriptional changes compared with 0.05 and 0.005 μM BPDE. Also the 0.05 μM BPDE elicited more changes in gene expression than the 0.005 μM dose such as in cell cycle genes. In correlation, the high-dose BPDE generated moderate cytotoxicity and provoked severe S and G_2/M phase cell cycle arrest, while the two lower doses did not impair cell viability evidently, but the medium dose still evoked apparent S and G_2/M phase cell cycle arrest in contrast to the low dose. Previously, Akerman et al. showed a high-dose (1 μM) BPDE that resulted in more than 50% cytotoxicity within 24 h induced tens of transcriptional changes in TK6 cells of several hundred genes spotted on a cDNA array, while two lower doses (0.1 and 0.01 μM) of BPDE with low cytotoxicity almost did not induce any transcriptional changes of these genes, though both of which also induced adducts and mutation [7]. These observations regarding cellular differential response to various levels of BPDE indicate that gene expression and phenotypic changes are tightly linked, and higher doses of toxicants would have deeper impact on both of which.

Cell division cycle is a highly coordinated machinery accompanied by complex transcriptional programs, which involve periodical expression of nearly one thousand genes (>850) according to the cell cycle phases [43]. A prominent observation of this study is that the expression of more than 150 of these cell cycle phase-related genes was modulated, and adapted to the cell cycle arrest phenotype after BPDE exposure (Table 1 and Supplementary Table 1). For example, histone genes are highly expressed in S phase under normal conditions [43], which implies that a naturally growing culture with more S phase cells in proportion would have higher expression of these genes. However, the expression of *H1F0* histone gene was less in 0.05 and 0.5 μM BPDE-treated cultures than control culture, though there were higher proportions of S phase cells in treated cultures. This down-regulation most likely accommodated with the S phase arrest induced by BPDE. A number of other genes such as that function in G_2/M phase were also regulated at early stage and adapted to the cell cycle arrest as described before. Other labs have also observed that expression of a few cell cycle genes including histone genes and cyclin genes were altered by BPDE damage and correlated with S and G_2/M phase arrest in different treatment and cell models [7,10–12]. Thus, disturbance of the periodically expressed cell cycle genes might be a common mechanism when establishing cell cycle arrest upon DNA damage.

BPDE was previously shown not to induce a G_1/S transition arrest in both normal and transformed cell types [10,12,44], as also found in a normal cell type in this study. Such a nature would presumably promote mutagenesis and genome instability due to permitting DNA synthesis on damaged templates [44]. An important finding in this study was that the expression of *CCNE1* and *CCNE2* was up-regulated upon 0.5 μM BPDE treatment. This modulation would overcome the negative effect of altered expression of *CDK6*, *CDKN1A* and *CDKN1C*, and promote the damaged cells entry into S phase. Thus, *CCNE1* and *CCNE2* may play a role in the G_1-arrest deficiency, and act as oncogenes in BPDE-induced mutagenesis and carcinogenesis.

Abundant genes related to cell growth and apoptosis were affected by the 0.5 μM BPDE treatment, e.g., the up-regulation of *GDF15*, *PEA15*, *ATF3*, *HEXIM1* and *SAT1*, and the down-regulation of *EGFR*, *IGF1R*, *PRKCA*, *ITPR1* and *MYC*, which generally indicated cellular damage, growth inhibition, and apoptotic tendency. The up-regulation of *ATF3* [8,12], *HEXIM1* [11] and *SAT1* [7], and down-regulation of *MYC* [7], had also been found in previous studies, indicating common mechanisms can exist in response to BPDE in different cell types.

Bioinformatic analysis of up-regulated genes has predicted the activation of stress response-related TFs including AP-1, ATF3, NF-κB, TP53, ELK1, CREB1, ATF4, ATF6, and etc. after BPDE exposure. Among which, activation of AP-1, ATF3, NF-κB, TP53 and ELK1 as well as related stress signaling pathways, e.g. MAPKs (ERKs, JNKs, and p38 MAPK), NF-κB, and ATM/ATR, by BPDE was previously reported [12,33–35], while the predicted activation of CREB1, ATF4, and ATF6 by BPDE, and its possible relation with ER stress pathway were not known before. The up-regulated genes were implicated in multiple functions including cell cycle, cell survival, signal transduction, RNA processing, cytoskeleton and metabolism, etc. These transcriptional changes and cross-talks among their related signaling pathways reflected the complexity of gene regulation in cellular response to chemical insults.

Gene ontology analysis of the microarray data using GSEA has identified the enrichment of genes implicated in cell cycle regulation, proliferation, apoptosis, signal transduction, transcription, RNA processing, protein metabolism, transport, cytoskeleton and DNA repair etc. (Supplementary Table 2). The alteration of these genes primarily indicated down-regulation of cell cycle, proliferation, transport, cytoskeleton and DNA repair after 0.5 μM BPDE exposure (Supplementary Fig. 1). In addition to above-mentioned quantitative RT-PCR-validated genes, other enriched gene categories identified by microarray may also have important relevance with cellular response to BPDE. Many cytoskeleton genes were also involved in cell cycle G_2/M phase, e.g., *KIF2C*, *KIF11*, *CENPF*, *MID1*, *TPX2*, *BUB1*, and etc. [43], indicating that down-regulation of cytoskeleton might be related to the cell cycle arrest induced by BPDE. The repression of transport genes such as *AP1S1*, *AP1G1*, *AGAP1*, *EEA1*, *KPNA1*, *KPNA3*, *KPNA6*, *KPNB1*, and etc., which played roles in vesicle-mediated and nucleocytoplasmic transport [45,46], was previously not noticed. The down-regulation of DNA repair genes such as *RAD23B*, *GTF2H1*, *GTF2H4*, *RAD50*, *RAD51C*, *TDG*, and etc. that function in nucleotide excision repair, homologous recombination or base excision repair [47], would possibly promote mutagenesis after BPDE-DNA damage [11]. All these expression changes and related biological meanings deserve further investigations.

In summary, this study revealed that BPDE exposure could induce early transcriptional changes and disturb multiple cellular processes, which parallel with cell cycle arrest and growth inhibition in a dose-dependent manner. Analysis of the function and regulation of the affected genes helped to understand how stress signaling pathways, transcription factors, and their target genes were coordinated in the cellular response to BPDE at early stage. The gene expression change levels induced by the dosage of BPDE used in this study were relatively low, and independent RNA samples were applied for the DNA microarray and real-time RT-PCR measurements, both of which may account for why only a part of differentially expressed genes observed by the microarray analysis was verified by the RT-PCR measurements. Further biological experiments are needed to elucidate what exact roles these differentially expressed genes and related pathways play in this chemical-induced effect. In addition, more meticulous analysis of gene expression patterns in a variety of cell types, and time-course comparison will help to generate a general model for cellular responses to genotoxic stress.

Materials and methods

Cell culture and chemical treatment

Benzo[a]pyrene diol epoxide ((±)-*anti*-BPDE) was obtained from the National Cancer Institute Chemical Carcinogen Reference Standard Repository (Kansas City, MO). BPDE stock solution was prepared in anhydrous dimethyl sulfoxide (DMSO) and used immediately. Human amnion epithelial FL cells were cultured in minimal essential medium (MEM, Gibco-Invitrogen, Carlsbad, CA) supplemented with 10% newborn bovine serum (Gibco-Invitrogen), 100 U/mL penicillin, and 100 μg/mL streptomycin in a humidified atmosphere of 5% CO_2 at 37 °C. For treatment, FL cells in logarithmic growth were exposed to various doses of BPDE or a DMSO solvent control in serum-free medium for 2 h. All cultures received an equal volume of DMSO (0.1%). Following the chemical exposure, the cultures were rinsed with Hank's buffer solution, and incubated in fresh serum-supplemented medium for additional time before harvest. The cytotoxicity of BPDE was determined with a MTT reduction assay using CellTiter 96® AQueous One Solution Cell Proliferation Assay Kit (Promega).

Microarray profiling and data analysis

For microarray study, duplicate cultures were treated with various concentrations (0, 0.005, 0.05, 0.5 μM) of BPDE for 2 h, respectively. At 4 h post treatment, cells were rinsed once with ice-cold phosphate buffered saline and lysed, total RNA was isolated with Trizol reagents (Invitrogen), and further purified using the RNeasy Mini Kit (Qiagen, Valencia, CA). The quality and quantity of RNA were assessed by denaturing agarose gel electrophoresis and spectrophotometric ultraviolet absorbance at 260/280 nm, respectively. Each of the generated RNA samples was measured by one Human Genome U133 Set array, which covers more than 39,000 transcripts and variants representing 33,000 well-substantiated human genes and expressed sequence tags. Microarray hybridization and detection was performed as described in the Affymetrix GeneChip Expression Analysis Technical Manual.

Microarray data analysis was performed according to the Affymetrix GeneChip® Expression Analysis (Data Analysis Fundamentals). The probe level data was processed using the MAS5.0 algorithm, and the average intensity of each array was globally scaled to a target of 500. The followed single-array and two-array comparison analysis generated detection call and change call for each probe set, respectively. For duplicated control and treatment microarrays, each probe set would possess four detection calls arisen from each microarray, and four change calls produced by the orthogonal comparisons between the control and treatment microarrays. The fold change of a probe set was calculated based on the signal log ratios resulted from two-array comparison analysis. The criteria of significantly differential expression for a probe set was: 1) it possessed at least one "Present" detection call in the single-array analysis, 2) it showed four consistent "Increase" or "Decrease" change calls (100% standard) or three consistent "Increase" or "Decrease" change calls plus one "No change" call (75% standard) in the two-array comparison analysis, and 3) the magnitude of fold change was more than 1.2.

The genes differentially expressed in at least one of the three doses of BPDE treatment were subjected to Cluster 3.0 software (Stanford University) for hierarchical cluster analysis using Pearson correlation (uncentered) distance metrics and average linkage cluster method. The cluster result was visualized with Java TreeView 1.0.13 software (Stanford University). Gene Set Enrichment Analysis (GSEA) was used to analyze the functional categories enrichment in the differentially expressed genes by comparing to the mSigDB gene ontology gene set collection (v2.5) (http://www.broad.mit.edu/gsea/msigdb/index.jsp) [48]. Individual gene sets were filtered out when enough of the members (by default 15–500 genes) were contained in the differentially expressed gene list. The enrichment degree of a filter-out gene set was denoted by the ratio relative to the gene set original size.

Quantitative real-time RT-PCR

Triplicate RNA samples were independently prepared for quantitative real-time RT-PCR analysis. Total RNA was isolated with Trizol reagents (Invitrogen), and all RNA samples were DNase-treated using the DNA-free™ Kit (Ambion, Austin, TX) to eliminate DNA contamination. RNA integrity was verified by 1% agarose gel electrophoresis and the quantity was determined by spectrophotometry. Single-strand cDNA was synthesized using the High-Capacity cDNA Archive Kit (Applied Biosystems, Foster City, CA). Quantitative real-time RT-PCR was performed using ABI TaqMan Low Density Arrays, which is a 384-well microfluidic card pre-loaded with optimised probes and matching primers for customer-selected genes. The reaction system in each well was about 2 μL, containing 1 ng cDNA template, 250 nM probe, 900 nM each of the primers, and TaqMan® Universal PCR Master Mix. The thermal cycling process was performed on an ABI Prism 7900HT Sequence Detection System, starting with 50 °C for 2 min and 94.5 °C for 10 min, and continuing with 40 cycles of 97 °C for 15 s and 59.7 °C for 30 s. Relative quantification analysis was performed with ABI Prism SDS 2.1.1 software. The endogenous control 18s rRNA was used to normalize differences in the input amount of total cDNAs. Normalized ΔCt values were then used to determine the statistical significance ($p<0.05$) of differential expression between

BPDE-exposed and control samples using Student's paired, two-tailed *t*-test. Fold changes were calculated using the comparative C_T method as described in the ABI Prism 7900HT SDS User Guide.

Cell cycle analysis

Cells in 6-well plate were treated with various concentrations (0, 0.005, 0.05, 0.5 μM) of BPDE. At different times (4, 13 and 22 h) post exposure, cells were harvested by trypsinization, fixed in 70% ice-cold ethanol at 4 °C for overnight, then washed and resuspended in PBS containing propidium iodide (20 μg/mL), RNaseA (50 μg/mL), and TritonX-100 (0.1%) at 37 °C for 30 min. Samples were then measured on a Coulter EPICS XL flow cytometer, and the post-acquisition list mode data was analyzed with WinMDI 2.8 software.

Bioinformatic analysis

The PAP (Promoter Analysis Pipeline) web application suite (http://bioinformatics.wustl.edu/webTools/portalModule/PromoterSearch.do) was used to analyze the TFBSs (transcription factor binding sites) in the promoter regions of the up-regulated genes [49]. It identifies specific TFBSs by calculating overrepresentation of characterized transcription factor binding profiles in the promoter sequences using weight matrices from TRANSFAC and JASPER databases. In current study, the identified TFBSs ($p<0.05$) were reciprocally used for determination of regulatory transcription factors for each gene.

Acknowledgments

We thank the reviewers for constructive and detailed comments. We thank Jun Yang for his help for this work. This research was supported by the grant 2002CB512901 from the National Basic Research Program of China.

Appendix A. Supplementary data

Supplementary data associated with this article can be found, in the online version, at doi:10.1016/j.ygeno.2008.12.007.

References

[1] G.N. Wogan, Markers of exposure to carcinogens, Environ. Health Perspect. 81 (1989) 9–17.
[2] W. Yang, Portraits of a Y-family DNA polymerase, FEBS Lett. 579 (2005) 868–872.
[3] S.J. Wei, et al., Dose-dependent differences in the profile of mutations induced by an ultimate carcinogen from benzo[a]pyrene, Proc. Natl. Acad. Sci. U. S. A. 88 (1991) 11227–11230.
[4] S.P. Hussain, et al., Mutability of p53 hotspot codons to benzo(a)pyrene diol epoxide (BPDE) and the frequency of p53 mutations in nontumorous human lung, Cancer Res. 61 (2001) 6350–6355.
[5] M.H. Tsai, et al., Transcriptional responses to ionizing radiation reveal that p53R2 protects against radiation-induced mutagenesis in human lymphoblastoid cells, Oncogene 25 (2006) 622–632.
[6] A. Pisarchik, J. Wortsman, A. Slominski, A novel microarray to evaluate stress-related genes in skin: effect of ultraviolet light radiation, Gene 341 (2004) 199–207.
[7] G.S. Akerman, et al., Gene expression profiles and genetic damage in benzo(a) pyrene diol epoxide-exposed TK6 cells, Mutat. Res. 549 (2004) 43–64.
[8] I. Belitskaya-Levy, M. Hajjou, W.C. Su, T.A. Yie, K.M. Tchou-Wong, M.S. Tang, J.D. Goldberg, W.N. Rom, Gene profiling of normal human bronchial epithelial cells in response to asbestos and benzo(a)pyrene diol epoxide (BPDE), J. Environ. Pathol. Toxicol. Oncol. 26 (2007) 281–294.
[9] Z. Yu, B.N. Ford, B.W. Glickman, Identification of genes responsive to BPDE treatment in HeLa cells using cDNA expression assays, Environ. Mol. Mutagen. 36 (2000) 201–205.
[10] S.L. Hockley, V.M. Arlt, G. Jahnke, A. Hartwig, I. Giddings, D.H. Phillips, Identification through microarray gene expression analysis of cellular responses to benzo(a)pyrene and its diol-epoxide that are dependent or independent of p53, Carcinogenesis 29 (2008) 202–210.
[11] W. Luo, W. Fan, H. Xie, L. Jing, E. Ricicki, P. Vouros, L.P. Zhao, H. Zarbl, Phenotypic anchoring of global gene expression profiles induced by N-hydroxy-4-acetylaminobiphenyl and benzo[a]pyrene diol epoxide reveals correlations between expression profiles and mechanism of toxicity, Chem. Res. Toxicol. 18 (2005) 619–629.
[12] A. Wang, et al., Response of human mammary epithelial cells to DNA damage induced by BPDE: involvement of novel regulatory pathways, Carcinogenesis 24 (2003) 225–234.
[13] G. Liu, Y. Yu, Endoplasmic reticulum stress is involved in N-methyl-N'-nitro-N-nitrosoguanidine, benzo[a]pyrene-7,8-dihydrodiol-9,10-epoxide and mitomycin-induced cellular response in FL cells, Chinese J. Pathophysiol. 22 (2006) 1–6.
[14] G. Liu, Y. Shang, Y. Yu, Induced endoplasmic reticulum (ER) stress and binding of over-expressed ER specific chaperone GRP78/BiP with dimerized epidermal growth factor receptor in mammalian cells exposed to low concentration of N-methyl-N'-nitro-N-nitrosoguanidine, Mutat. Res. 596 (2006) 12–21.
[15] J. Shen, M. Wu, Y. Yu, Proteomic profiling for cellular responses to different concentrations of N-methyl-N'-nitro-N-nitrosoguanidine, J. Proteome Res. 5 (2006) 385–395.
[16] T. Meergans, W. Albig, D. Doenecke, Varied expression patterns of human H1 histone genes in different cell lines, DNA Cell Biol. 16 (1997) 1041–1049.
[17] S. Dutertre, et al., Phosphorylation of CDC25B by Aurora-A at the centrosome contributes to the G2-M transition, J. Cell. Sci. 117 (2004) 2523–2531.
[18] A. Lindqvist, W. van Zon, C. Karlsson Rosenthal, R.M. Wolthuis, Cyclin B1-Cdk1 activation continues after centrosome separation to control mitotic progression, PLoS Biol. 5 (2007) e123.
[19] M. Okada, I.M. Cheeseman, T. Hori, K. Okawa, I.X. McLeod, J.R. Yates 3rd, A. Desai, T. Fukagawa, The CENP-H-I complex is required for the efficient incorporation of newly synthesized CENP-A into centromeres, Nat. Cell Biol. 8 (2006) 446–457.
[20] E.R. Kramer, C. Gieffers, G. Holzl, M. Hengstschlager, J.M. Peters, Activation of the human anaphase-promoting complex by proteins of the CDC20/Fizzy family, Curr. Biol. 8 (1998) 1207–1210.
[21] U. Gruneberg, R. Neef, X. Li, E.H. Chan, R.B. Chalamalasetty, E.A. Nigg, F.A. Barr, KIF14 and citron kinase act together to promote efficient cytokinesis, J. Cell Biol. 172 (2006) 363–372.
[22] T. Maney, M. Wagenbach, L. Wordeman, Molecular dissection of the microtubule depolymerizing activity of mitotic centromere-associated kinesin, J. Biol. Chem. 276 (2001) 34753–34758.
[23] N.J. Wells, N. Watanabe, T. Tokusumi, W. Jiang, M.A. Verdecia, T. Hunter, The C-terminal domain of the Cdc2 inhibitory kinase Myt1 interacts with Cdc2 complexes and is required for inhibition of G(2)/M progression, J. Cell. Sci. 112 (Pt 19) (1999) 3361–3371.
[24] K. Vermeulen, D.R. Van Bockstaele, Z.N. Berneman, The cell cycle: a review of regulation, deregulation and therapeutic targets in cancer, Cell Prolif. 36 (2003) 131–149.
[25] J. Schlessinger, Cell signaling by receptor tyrosine kinases, Cell 103 (2000) 211–225.
[26] T.J. Jang, N.I. Kim, C.H. Lee, Proapoptotic activity of NAG-1 is cell type specific and not related to COX-2 expression, Apoptosis 11 (2006) 1131–1138.
[27] H. Renganathan, H. Vaidyanathan, A. Knapinska, J.W. Ramos, Phosphorylation of PEA-15 switches its binding specificity from ERK/MAPK to FADD, Biochem. J. 390 (2005) 729–735.
[28] T. Hai, M.G. Hartman, The molecular biology and nomenclature of the activating transcription factor/cAMP responsive element binding family of transcription factors: activating transcription factor proteins and homeostasis, Gene 273 (2001) 1–11.
[29] M. Turano, G. Napolitano, C. Dulac, B. Majello, O. Bensaude, L. Lania, Increased HEXIM1 expression during erythroleukemia and neuroblastoma cell differentiation, J. Cell. Physiol. 206 (2006) 603–610.
[30] C.V. Dang, K.A. O'Donnell, K.I. Zeller, T. Nguyen, R.C. Osthus, F. Li, The c-Myc target gene network, Semin. Cancer Biol. 16 (2006) 253–264.
[31] E.B. Thompson, The many roles of c-Myc in apoptosis, Annu. Rev. Physiol. 60 (1998) 575–600.
[32] L. Li, J.N. Rao, B.L. Bass, J.Y. Wang, NF-kappaB activation and susceptibility to apoptosis after polyamine depletion in intestinal epithelial cells, Am. J. Physiol.: Gastrointest. Liver Physiol. 280 (2001) G992–G1004.
[33] J.J. Mukherjee, H.C. Sikka, Attenuation of BPDE-induced p53 accumulation by TPA is associated with a decrease in stability and phosphorylation of p53 and downregulation of NFkappaB activation: role of p38 MAP kinase, Carcinogenesis 27 (2006) 631–638.
[34] J. Li, et al., Differential effects of polycyclic aromatic hydrocarbons on transactivation of AP-1 and NF-kappaB in mouse epidermal cl41 cells, Mol. Carcinog. 40 (2004) 104–115.
[35] S. Chen, N. Nguyen, K. Tamura, M. Karin, R.H. Tukey, The role of the Ah receptor and p38 in benzo[a]pyrene-7,8-dihydrodiol and benzo[a]pyrene-7,8-dihydrodiol-9,10-epoxide-induced apoptosis, J. Biol. Chem. 278 (2003) 19526–19533.
[36] A.J. Shaywitz, M.E. Greenberg, CREB: a stimulus-induced transcription factor activated by a diverse array of extracellular signals, Annu. Rev. Biochem. 68 (1999) 821–861.
[37] L. Yue, S. Lu, J. Garces, T. Jin, J. Li, Protein kinase C-regulated dynamitin-macrophage-enriched myristoylated alanine-rice C kinase substrate interaction is involved in macrophage cell spreading, J. Biol. Chem. 275 (2000) 23948–23956.
[38] S.S. Mann, J.A. Hammarback, Gene localization and developmental expression of light chain 3: a common subunit of microtubule-associated protein 1A(MAP1A) and MAP1B, J. Neurosci. Res. 43 (1996) 535–544.
[39] Y. Wang, G. Tian, N.J. Cowan, F. Cabral, Mutations affecting beta-tubulin folding and degradation, J. Biol. Chem. 281 (2006) 13628–13635.
[40] C. Keshava, R.L. Divi, D.L. Whipkey, B.L. Frye, E. McCanlies, M. Kuo, M.C. Poirier, A. Weston, Induction of CYP1A1 and CYP1B1 and formation of carcinogen–DNA adducts in normal human mammary epithelial cells treated with benzo[a]pyrene, Cancer Lett. 221 (2005) 213–224.
[41] M. Schroder, R.J. Kaufman, ER stress and the unfolded protein response, Mutat. Res. 569 (2005) 29–63.

[42] G. Wang, Y. Yu, X. Chen, H. Xie, Low concentration N-methyl-N'-nitro-N-nitrosoguanidine activates DNA polymerase-beta expression via cyclic-AMP-protein kinase A-cAMP response element binding protein pathway, Mutat. Res. 478 (2001) 177–184.
[43] M.L. Whitfield, et al., Identification of genes periodically expressed in the human cell cycle and their expression in tumors, Mol. Biol. Cell 13 (2002) 1977–2000.
[44] Q.A. Khan, A. Dipple, Diverse chemical carcinogens fail to induce G(1) arrest in MCF-7 cells, Carcinogenesis 21 (2000) 1611–1618.
[45] M. Kohler, C. Speck, M. Christiansen, F.R. Bischoff, S. Prehn, H. Haller, D. Gorlich, E. Hartmann, Evidence for distinct substrate specificities of importin alpha family members in nuclear protein import, Mol. Cell. Biol. 19 (1999) 7782–7791.
[46] Z. Nie, M. Boehm, E.S. Boja, W.C. Vass, J.S. Bonifacino, H.M. Fales, P.A. Randazzo, Specific regulation of the adaptor protein complex AP-3 by the Arf GAP AGAP1, Dev. Cell 5 (2003) 513–521.
[47] R.D. Wood, M. Mitchell, T. Lindahl, Human DNA repair genes, 2005, Mutat. Res. 577 (2005) 275–283.
[48] A. Subramanian, et al., Gene set enrichment analysis: a knowledge-based approach for interpreting genome-wide expression profiles, Proc. Natl. Acad. Sci. U. S. A. 102 (2005) 15545–15550.
[49] L.W. Chang, B.R. Fontaine, G.D. Stormo, R. Nagarajan, PAP: a comprehensive workbench for mammalian transcriptional regulatory sequence analysis, Nucleic Acids Res. 35 (2007) W238–W244.